J_ID: AR Customer A_ID: AR23646 Cadmus Art: AR23646 Ed. Ref. No.: AR-17-0026.R1 Date: 8-August-17 Stage: Page: 1

Morphology and Postnatal Development of Lower Hindlimbs in *Desmodus rotundus* (Chiroptera: Phyllostomidae): A Comparative Study

NICOLÁS REYES-AMAYA,[1]* ADRIANA JEREZ,[2] AND DAVID FLORES[1,3]

[1]Unidad Ejecutora Lillo (CONICET—Fundación Miguel Lillo)
San Miguel de Tucumán 4000, Argentina
[2]Laboratorio de Ecología Evolutiva, Departamento de Biología,
Facultad de Ciencias, Universidad Nacional de Colombia, Sede Bogotá, Colombia
[3]Instituto de Vertebrados, Fundación Miguel Lillo,
San Miguel de Tucumán 4000, Argentina

ABSTRACT

The hindlimbs in bats are functionally adapted to serve as a hook to attach to the mother from birth, and to roost during independent life. Although bats exhibit different terrestrial locomotion capabilities involving hindlimbs, hindlimb morphology and postnatal development have been poorly studied. We describe in detail the postnatal development and bone morphology of hindlimbs of the nimble walker vampire bat, *Desmodus rotundus*, and compare adult characters with the insectivorous *Molossus molossus* (erratic walker) and the frugivorous *Artibeus lituratus* (non-walker). The advanced ossification of most hindlimb elements of *D. rotundus* at the newborn stage is consistent with the functional role of this structure at birth in bats. The development completion events of hindlimb bone elements and bone processes in *D. rotundus* coincide with the cranial bone processes completion and suture closure events. Those events occur when individuals begin to feed by themselves. There are differences in the number and position of bone processes and sesamoids in adults among the compared species, most of which are described for the first time, and in the case of *D. rotundus* and *M. molossus* mostly related to a greater and tight articulation between elements. These facts seem to be closely associated with the different terrestrial locomotion capabilities, and in the case of the exclusively sanguivorous *D. rotundus* with specializations for obtaining food. Anat Rec, 00:000–000, 2017. © 2017 Wiley Periodicals, Inc.

Key words: bone processes; ossification; sesamoids; terrestrial locomotion; vampire bat

Mammals possess a broad spectrum of locomotion strategies, with bats (Chiroptera) being the only group that has developed active flight, and exhibiting a particular body plan associated with this skill (Walton and Walton, 1970; Scholey, 1986). Limbs of bats exhibit a trade-off between adequate structural support and reduced weight for flight, involving particular morphological patterns, such as bone reductions (Vaughan, 1970), joint rotations (MacAlister, 1872; Vaughan, 1959),

Grant sponsor: Agencia Nacional de Promoción Científica y Tecnológica, Argentina (CONICET); Grant number: PICT2012-1583.

*Correspondence to: Nicolás Reyes-Amaya, Fundación Miguel Lillo, Miguel Lillo 251, 4° floor, CP4000, San Miguel de Tucumán, Tucumán, Argentina. E-mail: nicolas.reyes2@gmail.com

Received 30 January 2017; Revised 30 May 2017;
Accepted 16 June 2017.

DOI 10.1002/ar.23646
Published online 00 Month 2017 in Wiley Online Library (wileyonlinelibrary.com).

J_ID: **AR** Customer A_ID: **AR23646** Cadmus Art: **AR23646** Ed. Ref. No.: **AR-17-0026.R1** Date: **8-August-17** Stage: Page: **2**

passive digital lock (Schutt, 1993), and the presence of a calcar bone in some species (Schutt and Simmons, 1998).

The New World leaf-nosed bats (Phyllostomidae) possess the greatest morphological and dietary variations among mammals, with feeding habits compassing carnivory, insectivory, omnivory, nectarivory, frugivory and sanguivory (Baker et al., 2012). This wide range of feeding habits makes this family a model group for the study of adaptive morphological changes related to the natural history of their species. Sanguivory represents one of the most specialized diets among mammals and is present only in the true vampire bats: *Desmodus rotundus*, *Diaemus youngii*, and *Diphylla ecaudata* (Desmodontinae: Phyllostomidae), which exhibit morphological, physiological and behavioral characters associated with their diet (Greenhall and Schmidt, 1988; Ferrarezzi and Gimenez, 1996; Mollerach and Mangione, 2004).

The association of terrestrial locomotion as a specialization related to diet in *D. rotundus* has been widely recognized (Altenbach, 1979; Greenhall and Schmidt, 1988; Hand et al., 2009). Because this species feeds on animals that widely exceed its size and weight, the agile locomotion on land constitutes an advantage to avoid damage and even death during feeding (Altenbach, 1979; Riskin et al, 2006; Hand et al., 2009). Terrestrial locomotion in adult bats has been classified by Vaughan (1970) into three categories: bats that cannot walk; bats that walk through erratic movements, and bats that walk nimbly. The common vampire bat (*D. rotundus*) is able to walk nimbly, jump and run (Altenbach, 1979; Schutt et al., 1997; Riskin and Hermanson, 2005), which makes this species an ideal model for functional interpretations based on locomotory aspects (Altenbach, 1979).

Although morphology and prenatal development of bat forelimbs has been widely studied and compared in several species (e.g., Sears et al., 2006; Adams, 2008; Adams and Shaw, 2013), hindlimb morphology and its postnatal development have been poorly studied (Adams and Thibault, 2000; Farnum et al., 2007; Koyabu and Son, 2014). Previous works have paid little attention to differences in characters between juveniles and adults, because the juvenile period is an ephemeral part of the life cycle, and occasionally hard to measure (Werner, 1999). In this report we provide a detailed description of the bone morphology and development at the hindlimbs of the nimble walker *D. rotundus* through a postnatal ontogenetic series, also providing data of morphometric changes in the proportional size of hindlimb regions. The adult characteristics were further compared with two other bat species with different ecological habits and terrestrial locomotion capabilities: the insectivorous and erratic walker *Molossus molossus* (Molossidae), and the frugivorous non-walker *Artibeus lituratus* (Phyllostomidae). Our principal aim was to detect general relationships in form and function of the hindlimb within particular life histories of these species; we expected that the hindlimb morphology and development in *D. rotundus* would reflect its terrestrial habits.

MATERIALS AND METHODS

Sampling and Processing of Specimens

For the description of postnatal development of hindlimbs in *D. rotundus*, 12 specimens of a complete development series were used. For the description of comparative hindlimb morphology in adults of species with different terrestrial locomotion capabilities, we studied five specimens of the nimble walker *D. rotundus*, three of the erratic walker *M. molossus* (Molossidae) and two of the non-walker *A. lituratus* (Phyllostomidae) (Table 1). The specimens were borrowed from Alberto Cadena Garcia Mammal Collection at the Instituto de Ciencias Naturales—Universidad Nacional de Colombia (ICN), and the Mammal Collection at the Museo Argentino de Ciencias Naturales Bernardino Rivadavia (MACN). The specimens were cleared and double-stained for observation of cartilage and bone, according to Wassersug (1976). We did not attempt to evaluate sex as a variation source due to the small sample size. T1

Anatomical Nomenclature and Age Categories

For all descriptions, nomenclature of bones, bone processes and sesamoids followed Schaller (2007) and Nomina Anatomica Veterinaria (NAV, 2012). The regions described correspond to the lower hindlimb: zeugopodium (zp: tibia and fibula) and autopodium (ap), the latter being composed of basipodium (bp: tarsals), metapodium (mp: metatarsals) and acropodium (acp: phalanges). Because the exact age was unknown, the postnatal developmental stages were determined following Reyes-Amaya and Jerez (2013), based on morphological (suture closure), morphometric (forearm length) and reproductive (sexual maturity) characters. Four age categories (newborn to adult) were considered, including eight stages of development (A to H): newborn (A, $n = 1$), juvenile (B, $n = 1$; C, $n = 1$; D, $n = 1$; E, $n = 1$), subadult (F, $n = 1$; G, $n = 1$), and adult (H, $n = 5$) (Table 1).

Ossification sequence and greatest changes in shape, position, and spatial relationship among bony elements were described for the postnatal development of *D. rotundus*, as well as general changes in the shape of the hindlimb and the zeugopodium/autopodium ratio (zp/ap). In addition, *D. rotundus* adult hindlimb bone morphology was comparatively described with respect to *M. molossus* and *A. lituratus*. In such comparison, the shape, position and spatial relationship among elements were also studied, as well as the general differences in zp/ap ratio, associating such aspects with the different walking abilities of these species. All descriptions were made via stereomicroscope observations.

RESULTS

Postnatal Development of Hindlimbs in *D. rotundus*

Stage A (newborn). All elements are in advanced ossification at birth, except for the calcar (Table 2) and sesamoids (Table 3). A zeugopodium/autopodium ratio (zp/ap) of 0.74 indicates an autopodium bigger than zeugopodium, conferring a short and robust appearance to the hindlimb (Table 5). T2 T3 T5

Zeugopodium. The diaphyses of the tibia and fibula are already ossified, whereas their epiphyses remain in ossification process, presenting a secondary ossification centre (except for the proximal epiphysis of the fibula; Fig. 1A,B and Table 2). The tibia is a robust cylindrical bone, whereas the fibula is thin and compressed at the dorso-ventral axis. F1

ID: **jwweb3b2server** Time: 14:50 I Path: D:/Wiley/Support/XML_Signal_Tmp_AA/JW-AR##170103

J_ID: **AR** Customer A_ID: **AR23646** Cadmus Art: **AR23646** Ed. Ref. No.: **AR-17-0026.R1** Date: **8-August-17** Stage: Page: **3**

TABLE 1. Specimens of *Desmodus rotundus*, *Molossus molossus*, and *Artibeus lituratus* analyzed in this study

Species	Specimen ID.	Age categories	Stages of development	Definition
D. rotundus	ICN in process (NR 024)	Newborn	A	Fa= 19.4 mm; Attached to the mother; Sutura interfrontalis and Sutura sagittalis being closed, but remain unfused.
	ICN in process (JLF 023)	Juvenile	B	Fa = 21.5 mm; Sutura premaxilolacrimalis appear completely closed and fused.
	ICN 21932		C	Fa = 28.6 mm; Sutura interparietalis and parietointerparietalis being closed, but remain unfused.
	ICN 21929		D	Fa = 38.5 mm; Sutura occipitointerparietalis being closed, but remain unfused.
	ICN 21933		E	Fa = 42.7 mm; Sutura frontonasalis, interfrontalis, maxilloincisiva, squamosa and occipitalis being closed, but remain unfused; Sutura interparietalis appear completely closed and fused.
	ICN 21926	Subadult	F	Fa = 49.1 mm; Free-living; Sutura frontopremaxillaris, interpremaxillaris, premaxillonasalis, zigomaticomaxillaris, zigomaicotemporalis, frontoparietalis and exoccipitoparietalis being closed, but remain unfused; Sutura frontalis, interfrontalis, internasalis, maxillolacrimalis, maxilloincisiva, sagittalis, occipitalis and parietointerparietalis appear completely closed and fused.
	ICN 21930		G	Fa = 56.8 mm; Sutura frontonasalis, frontopremaxillaris, interpremaxillaris, premaxillonasalis, zigomaticomaxillaris, frontoparietalis, exoccipitoparietalis, squamosa, zigomaticotemporalis, occipitointerparietalis and exoccipitosquamous suture appear completely closed and fused, completing the closure and fusion of all cranial sutures.
	ICN 21927 ICN 21928 ICN 21931 ICN 21934 ICN 21935	Adult	H	Fa = 61.2–65 mm; All sutures closed and fused; Presence of sexual activity (males with scrotal testicles, pregnant and lactating females); all cranial bone processes present and well developed: pfp, nc, op, pc, sc.
M. molossus	ICN in process (NR 038) ICN in process (NR 039) MACN 14147	Adult	H	Fa = 38.5–49 mm; All sutures closed and fused; Presence of sexual activity (males with scrotal testicles, pregnant and lactating females); all cranial bone processes present and well developed.
A. lituratus	ICN D0149 MACN 18426	Adult	H	Fa = 62–70 mm; All sutures closed and fused; Presence of sexual activity (males with scrotal testicles, pregnant and lactating females); all cranial bone processes present and well developed.

Definition of stages of development *sensu* Reyes-Amaya and Jerez (2013). Abbreviations: Fa, forearm length; pfp, preorbital frontal process; nc, nuchal crest; op, occipital process; pc, postorbital constriction; sc, sagital crest. For specimens in inclusion process by scientific collections, the number of field collection is given in parenthesis.

ID: **jwweb3b2server** Time: 14:50 I Path: D:/Wiley/Support/XML_Signal_Tmp_AA/JW-AR##170103

J_ID: **AR** Customer A_ID: **AR23646** Cadmus Art: **AR23646** Ed. Ref. No.: **AR-17-0026.R1** Date: **8-August-17** Stage: Page: **4**

TABLE 2. Ossification sequence of hindlimb bony elements in a postnatal series of *Desmodus rotundus*

Region		Bony elements	Prenatal	Newborn	Juvenile				Subadult		Adult
				A	B	C	D	E	F	G	H
Zeugopodium		Fibula	x								x
		Tibia	x							x	
Autopodium	Basipodium	Calcar					x	x			
		Talus	x				x				
		Calcaneus	x				x				
		Navicular	x				x				
		Cuneiform I	x				x				
		Cuneiform II	x				x				
		Cuneiform III	x				x				
		Cuboid	x				x				
	Metapodium	Metatarsal I	x			x					
		Metatarsal II	x			x					
		Metatarsal III	x			x					
		Metatarsal IV	x			x					
		Metatarsal V	x			x					
	Acropodium	Proximal phalanx I	x			x					
		Proximal phalanx II	x			x					
		Proximal phalanx III	x			x					
		Proximal phalanx IV	x			x					
		Proximal phalanx V	x			x					
		Medial phalanx II	x		x						
		Medial phalanx III	x		x						
		Medial phalanx IV	x		x						
		Medial phalanx V	x		x						
		Distal phalanx I	xx								
		Distal phalanx II	xx								
		Distal phalanx III	xx								
		Distal phalanx IV	xx								
		Distal phalanx V	xx								

For each bony element, the first appearance of the "x" symbol indicates the first inkling of ossification. The second appearance of the "x" symbol indicates end of ossification, including the closure of secondary ossification centres, if present.

TABLE 3. Ossification sequence of hindlimb sesamoids in a postnatal series of *Desmodus rotundus*

Region		Sesamoids	Newborn	Juvenile				Subadult		Adult
			A	B	C	D	E	F	G	H
Autopodium	Basipodium	Cuneiform I ventral sesamoid.*				x			x	
	Metapodium	Metatarsal V ventral sesamoid.*				x x				
		Ossa sesamoidea proximalia (paired), ventral and distal at metatarsals I–V.		x				x		
	Acropodium	Ossa sesamoidea dorsalia, dorsal and distal at proximal phalanx I/dorsal and proximal at medial phalanx II–V.			x				x	
		Ossa sesamoidea dorsalia, dorsal and distal at medial phalanx II and III.					x		x	
		Ossa sesamoidea dorsalia, dorsal and distal at medial phalanx IV and V.						x	x	

Sesamoids without name given previously in the literature are indicated with an asterisk. For each sesamoid, the first appearance of the "x" symbol indicates the first inkling of ossification. The second appearance of the "x" symbol indicates end of ossification.

ID: **jwweb3b2server** Time: 14:50 I Path: D:/Wiley/Support/XML_Signal_Tmp_AA/JW-AR##170103

J_ID: AR Customer A_ID: AR23646 Cadmus Art: AR23646 Ed. Ref. No.: AR-17-0026.R1 Date: 8-August-17 Stage: Page: 5

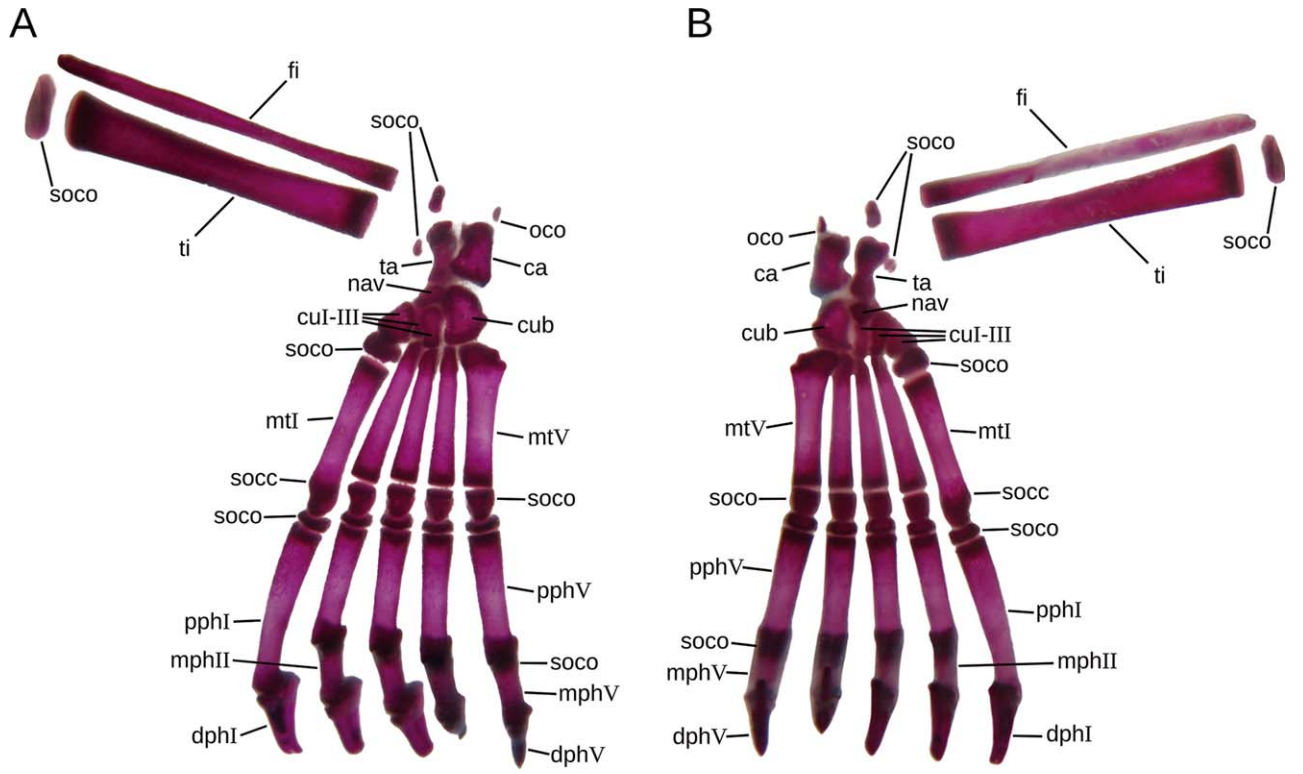

Fig. 1. Cleared and double-stained hindlimbs of D. rotundus at newborn stage of development. A, dorsal view. B, ventral view. Abbreviations: ca, calcaneus; cub, cuboid; cuI-III, cuneiforms I to III; dphI, distal phalange I; dphV, distal phalange V; fi, fibula; mphII, medial phalange II; mphV, medial phalange V; mtI, metatarsal I; mtV, metatarsal V; nav, navicular; pphI, proximal phalange I; pphV, proximal phalange V; soco, secondary ossification centre open; oco, ossification centre open; ta, talus; ti, tibia.

TABLE 4. Formation sequence of hindlimb bone processes and grooves in a postnatal series of *Desmodus rotundus*

Region	Bone processes	Newborn	Juvenile				Subadult		Adult
		A	B	C	D	E	F	G	H
Zeugopodium	Tibial ventral groove.*			x			x		
	Tibial medial groove.*				x		x		
	Fibular dorsal groove.*			x			x		
	Fibular ventral groove.*				x		x		
Autopodium Basipodium	Trochlea tali proximalis, lateral and proximal at the talus.		x		x				
	Tuber calcanei, medial and proximal at the calcaneus.		x		x				
	Talus dorsal process.*			x			x		
	Calcaneous dorsal process.*		x		x				
	Navicular ventral process.*		x		x				
Metapodium	Metatarsal V proximal process.*		x	x					

Bone processes without name given previously in the literature are indicated with an asterisk. For each bone process, the first appearance of the "x" symbol indicates start of formation. The second appearance of the "x" symbol indicates end of formation.

Autopodium. At the basipodium level, all elements are still in ossification process (Table 2). The calcaneus is the only element at the basipodium with an extra ossification centre, located at its proximal tip. The talus is rectangular, with a central constriction, whereas the calcaneus and navicular are triangular (Fig. 1A,B).

ID: jwweb3b2server Time: 14:50 I Path: D:/Wiley/Support/XML_Signal_Tmp_AA/JW-AR##170103

J_ID: **AR** Customer A_ID: **AR23646** Cadmus Art: **AR23646** Ed. Ref. No.: **AR-17-0026.R1** Date: **8-August-17** Stage: Page: **6**

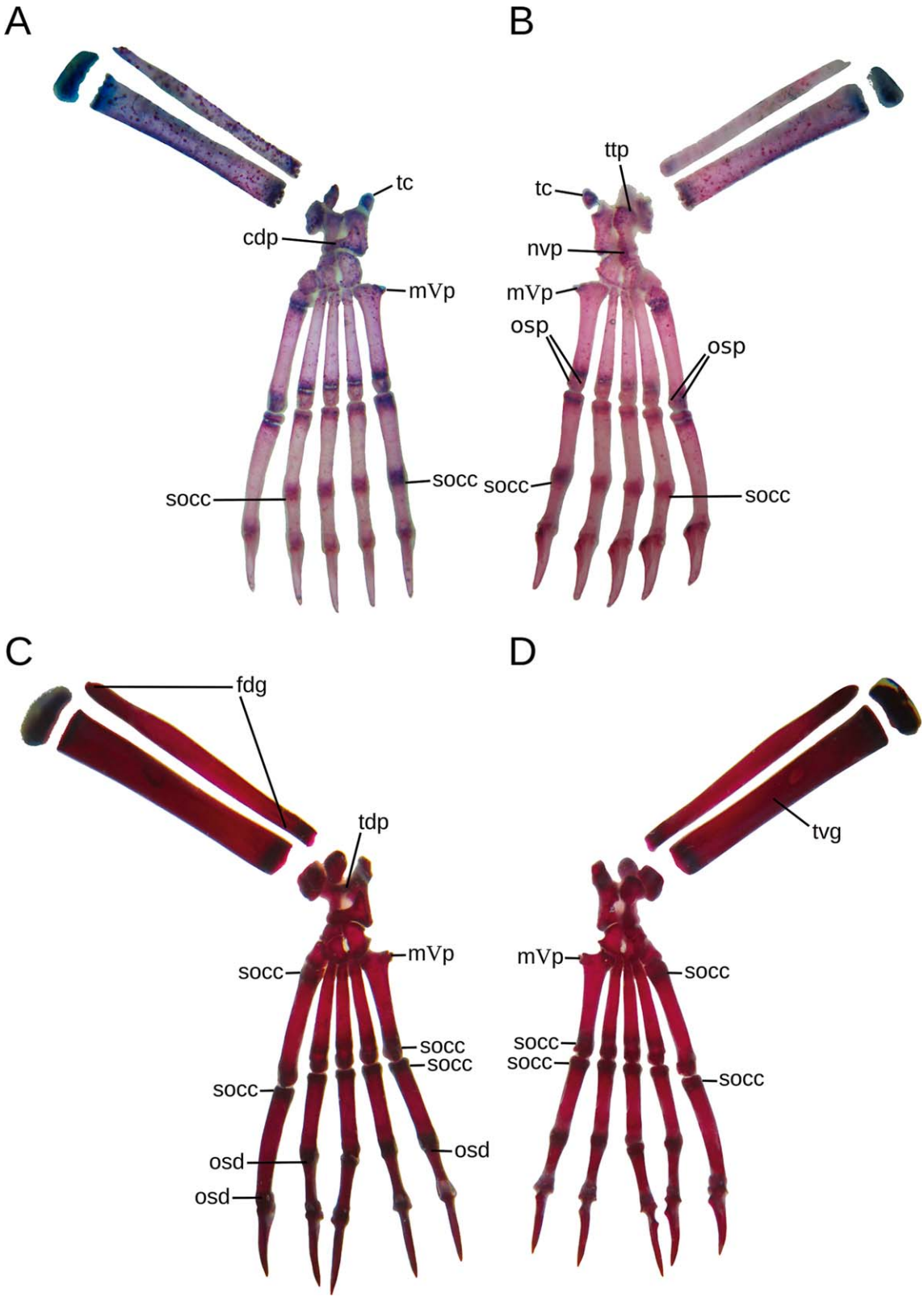

Fig. 2. Cleared and double-stained hindlimbs of D. rotundus. A and B, dorsal and ventral views of juvenile B stage of development. C and D, dorsal and ventral view of juvenile C stage of development. Abbreviations: cdp, calcaneous dorsal process; fdg, fíbular dorsal groove; mVp, metatarsal V proximal process; nvp, navicular ventral process; osd, Ossa sesamoidea dorsalia; osp, Ossa sesamoidea proximalia; socc, secondary ossification centre closed (ossification completion); tc, Tuber calcanei; tdp, talus dorsal process; ttp, Trochlea tali proximalis; tvg, tibial ventral groove.

J_ID: **AR** Customer A_ID: **AR23646** Cadmus Art: **AR23646** Ed. Ref. No.: **AR-17-0026.R1** Date: **8-August-17** Stage: Page: **7**

TABLE 5. Zeugopodium/autopodium length ratio in a postnatal series of *Desmodus rotundus*

Age categories	Stage of development	Zeugopodium		Autopodium		zp/ap ratio
Newborn	A (ICN in process - NR 024)	10.49		14.09		0.74
Juvenile	B (ICN in process - JLF 023)	11.20		15.20		0.74
	C (ICN 21932)	12.74		16.25		0.78
	D (ICN 21929)	15.21		16.21		0.94
	E (ICN 21933)	16.50		16.28		1.01
Subadult	F (ICN 21926)	21.34		16.57		1.29
	G (ICN 21930)	22.34		16.38		1.36
Adult	H (ICN 21927)	25.96	24.45	18.17	16.77	1.46
	H (ICN 21928)	24.45	(average)	17.15	(average)	
	H (ICN 21931)	23.58		16.35		
	H (ICN 21934)	24.05		15.27		
	H (ICN 21935)	24.23		16.92		

Collection ID of the specimens is given in parentheses. Abbreviations: zp, zeugopodium; ap, autopodium. Measurements in millimeters.

Cuneiform I and II are triangular. Cuneiform III is rectangular, whereas the cuboid is irregularly shaped, slightly circular. The proximity of cuneiform I and III displaces ventrally the position of cuneiform II at the dorso-ventral axis (Fig. 1B). At the metapodium level, all elements are still in ossification process (Table 2). The diaphyses of metatarsals I–V are already ossified, whereas the proximal epiphysis of metatarsal I, and the distal epiphyses of metatarsal II–V present a secondary ossification centre (Fig. 1A,B and Table 2). The distal epiphysis of the metatarsal I shows evidence of having recently fused to the diaphysis, evidencing the previous existence of a secondary ossification centre in this position (Fig. 1A,B). At the acropodium level, the diaphyses of all proximal and medial phalanges are already ossified, whereas their proximal epiphyses present a secondary ossification centre. The proximal phalanx of the digit I is elongated, conferring this digit a length nearly equal to the other digits. Distal phalanges are completely ossified and morphologically modified to support a thick keratinized claw (Fig. 1A,B and Table 2).

Stage B (juvenile). The bones have increased in size, but the hindlimb retain the same zp/ap ratio as in the previous stage (0.74; Table 5).

Zeugopodium. The most significant change is observed at the tibia, which is slightly depressed.

Autopodium. At the basipodium level, the *Trochlea tali proximalis* process begins to develop at the proximal end of the talus (Fig. 2B and Table 4), appearing as a convex thickening that articulates laterally with the tibia and fibula. The calcaneus initiates the formation of two processes, the first is the *Tuber calcanei*, located medially at the proximal tip of the calcaneus, as a spur-shaped projection that extends medially, product of the proximal extra ossification centre already mentioned in the previous development stage (Fig. 2A,B and Table 4). The second is a distal and dorsal process (called here as calcaneous dorsal process; Fig. 2A and Table 4), extending laterally as a thick arc on the dorsum of the talus. The navicular initiates the formation of a ventral and proximal process (called here as navicular ventral process; Fig. 2B and Table 4), which extends proximally over the ventral surface of the talus. At the metapodium level, each metatarsal shows on the ventral surface of its distal epiphyses a pair of cartilaginous sesamoids starting ossification, called *Ossa sesamoidea proximalia* (Fig. 2B and Table 3). Metatarsal V initiates the formation of a process at its proximal epiphysis (called here as metatarsal V proximal process; Fig. 2A,B and Table 4), which extends and widens medially and laterally. At the acropodium level, all the medial phalanges show their proximal epiphyses fused to the diaphyses, marking the end of ossification for these elements (Fig. 2A,B and Table 2).

Stage C (juvenile). A small variation of the zp/ap ratio is observed (0.78; Table 5).

Zeugopodium. The tibia presents a longitudinal groove along its ventral surface (called here as tibial ventral groove; Fig. 2D and Table 4), whereas the fibula presents a groove from the dorso-proximal to the latero-distal tip (called here as fibular dorsal groove; Fig. 2C and Table 4).

Autopodium. At the basipodium level, a proximal and medial process begins to develop at the dorsum of the talus, extending medially and articulating with the calcaneus (called here as talus dorsal process Fig. 2C and Table 4). At the metapodium level, the proximal epiphysis of metatarsal I and the distal epiphyses of metatarsals II–V are fused with the diaphyses, marking the end of ossification for these elements (Fig. 2C,D and Table 2). Metatarsal V proximal process is completely developed (Fig. 2C,D and Table 4). At the acropodium level, the proximal epiphyses of proximal phalanges I–V are fused with the diaphyses, marking the end of ossification for these elements (Fig. 2C,D and Table 2). Dorsally, the distal epiphysis of the proximal phalanx I and the proximal epiphyses of medial phalanges II–V exhibit the *Ossa sesamoidea dorsalia* as a cartilaginous sesamoid starting ossification (Fig. 2C and Table 3).

Stage D (juvenile). The zp/ap ratio (0.94; Table 5) indicates a zeugopodium that almost reaches the autopodium length.

Zeugopodium. The proximal epiphisis of the fibula has begun its ossification, presenting a secondary ossification centre (Fig. 3A,B). The tibia exhibits an additional longitudinal groove along its medial surface (called here as tibial medial groove; Fig. 3A,B and Table 4), whereas the fibula exhibits an additional longitudinal

ID: **jwweb3b2server** Time: 14:51 I Path: D:/Wiley/Support/XML_Signal_Tmp_AA/JW-AR##170103

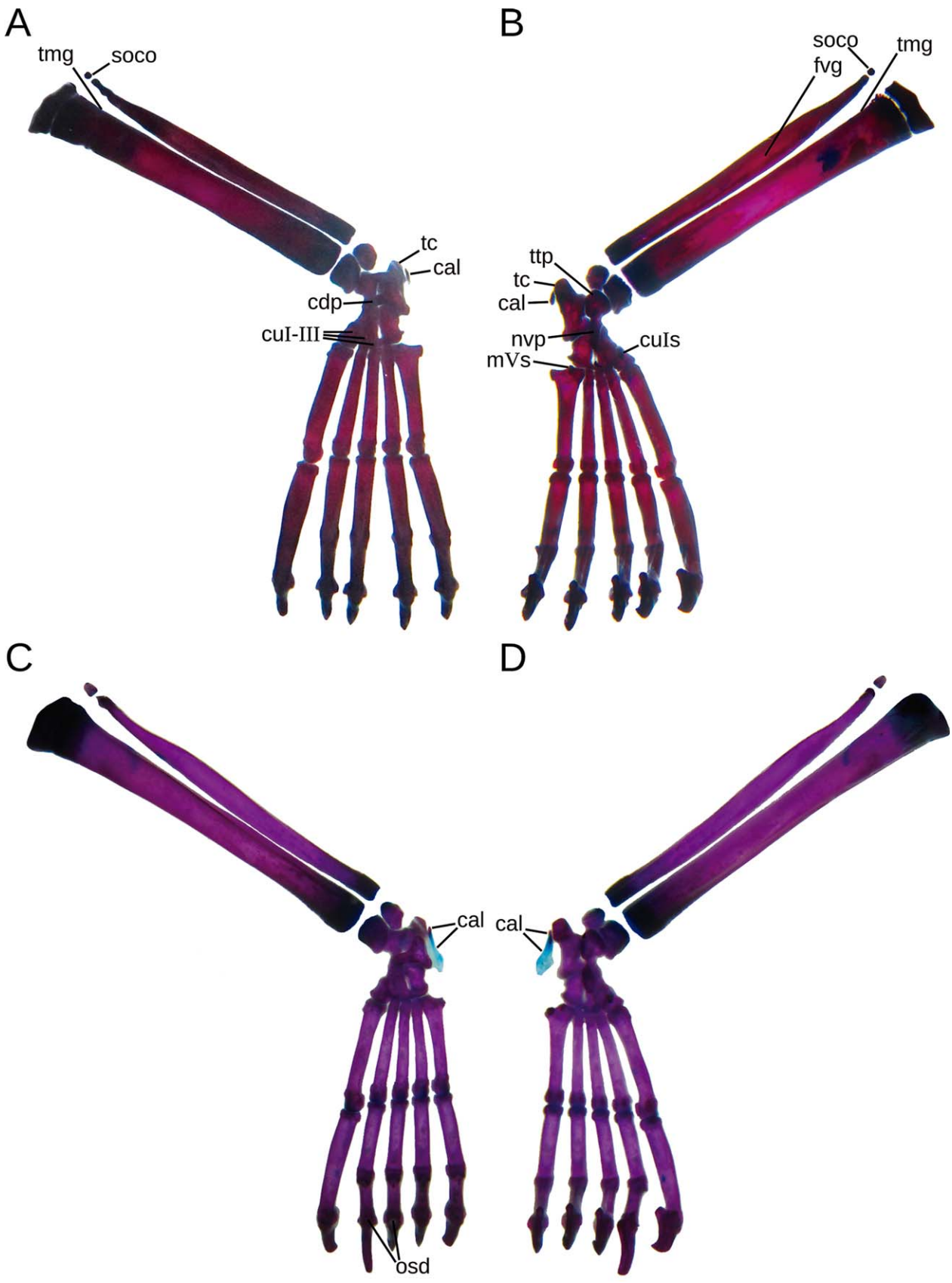

Fig. 3. Cleared and double-stained hindlimbs of D. rotundus. A and B, dorsal and ventral views of juvenile D stage of development. C and D, dorsal and ventral view of the juvenile E stage of development. Abbreviations: cal, calcar; cdp, calcaneous dorsal process; cul-III, cuneiforms I to III; culs, cuneiform I ventral sesamoid; fvg, fibular ventral groove; mVs, metatarsal V ventral sesamoid; nvp, navicular ventral process; osd, Ossa sesamoidea dorsalia; soco, secondary ossification centre open; tc, Tuber calcanei; tmg, tibial medial groove; ttp, Trochlea tali proximalis.

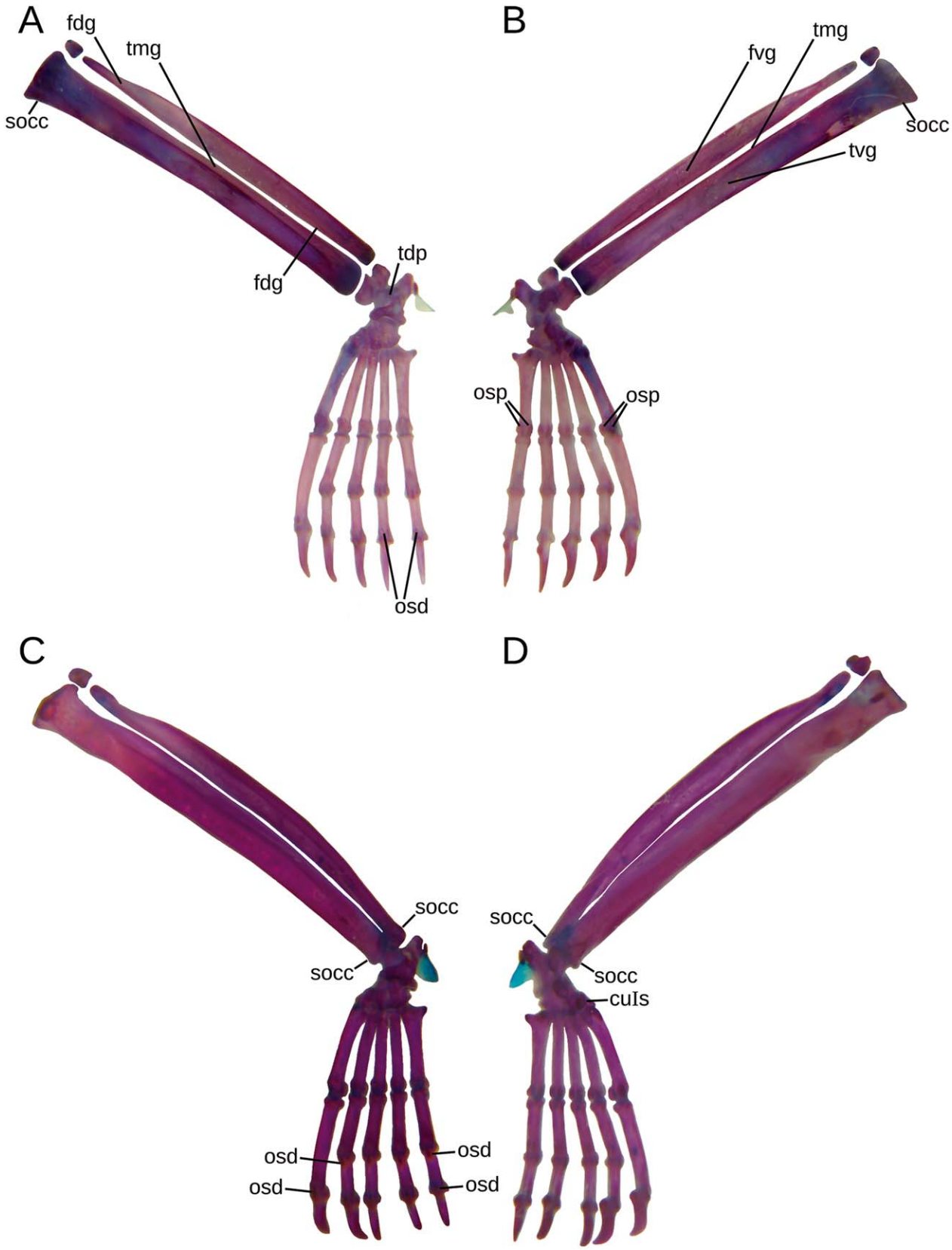

Fig. 4. Cleared and double-stained hindlimbs of D. rotundus. A and B, dorsal and ventral view of subadult F stage of development. C and D, dorsal and ventral view of subadult G stage of development. Abbreviations: culs, cuneiform I ventral sesamoid; fdg, fibular dorsal groove; fvg, fibular ventral groove; osd, Ossa sesamoidea dorsalia; osp, Ossa sesamoidea proximalia; socc, secondary ossification centre closed; tdp, talus dorsal process; tmg, tibial medial groove; tvg, tibial ventral groove.

J_ID: AR Customer A_ID: AR23646 Cadmus Art: AR23646 Ed. Ref. No.: AR-17-0026.R1 Date: 8-August-17 Stage: Page: 10

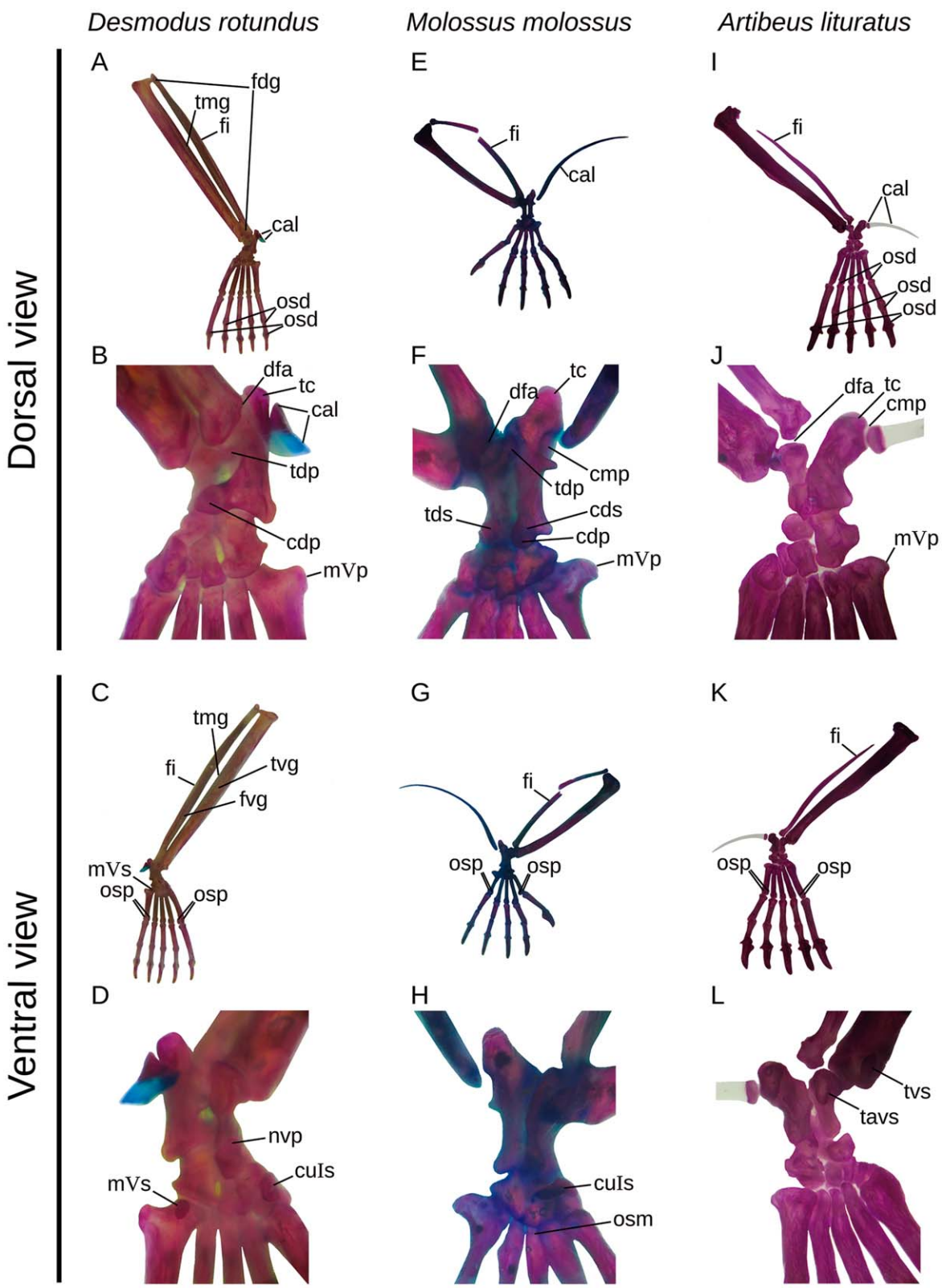

Fig. 5

J_ID: **AR** Customer A_ID: **AR23646** Cadmus Art: **AR23646** Ed. Ref. No.: **AR-17-0026.R1** Date: **8-August-17** Stage: Page: **11**

groove along its ventral surface (called here as fibular ventral groove; Fig. 3B and Table 4).

Autopodium. At the basipodium level, the talus, calcaneus and navicular are completely ossified and contains fully developed processes (except for the talus dorsal process; Table 4); these processes are the *Trochlea tali proximalis* (at the talus), *Tuber calcanei* (at the calcaneus), calcaneous dorsal process, and navicular ventral process (Fig. 3A,B and Table 4). The calcar is visible for the first time (Table 2) as a small rudimentary bone located medially next to, but not in contact with, the *Tuber calcanei* process (Fig. 3A,B). Cuneiforms I-III are completely ossified (Fig. 3A and Table 2). Cuneiform I exhibits a sesamoid starting ossification on its ventral surface (called here as cuneiform I ventral sesamoid; Fig. 3B and Table 3). At the metapodium level, metatarsal V exhibits an already ossified sesamoid on the ventral surface of its proximal epiphysis (called here as metatarsal V ventral sesamoid; Fig. 3B and Table 3).

Stage E (juvenile). The zp/ap ratio (1.01; Table 5) indicates a zeugopodium that equals the autopodium length.

Zeugopodium. The proximal epiphysis of the tibia begins to fuse with the diaphysis.

Autopodium. At the basipodium level, the calcar is completely developed; it appears as a small tab-like structure, retaining much of its distal extension in cartilaginous state (Fig. 3C,D and Table 2). At the acropodium level, the distal epiphyses of medial phalanges II and III exhibit on its dorsal surface the *Ossa sesamoidea dorsalia*, which is starting ossification (Fig. 3C and Table 3).

Stage F (subadult). The zp/ap ratio (1.29; Table 5) indicates a zeugopodium that exceeds the autopodium length, giving the limb a slender appearance.

Zeugopodium. The proximal epiphysis of the tibia is now fused to its diaphysis (Fig. 4A,B). The tibial and fibular grooves are completely developed, showing its final depth and emphasizing the T-shaped cross section of the shafts (Fig. 4A,B and Table 4). F4

Autopodium. At the basipodium level, the talus dorsal process is completely developed (Fig. 4A and Table 4). At the metapodium level, the *Ossa sesamoidea proximalia* are completely ossified (Fig. 4B and Table 3). At the acropodium level, the distal epiphyses of medial phalanges IV and V present the *Ossa sesamoidea dorsalia*, which is starting ossification (Fig. 4A and Table 3).

Stage G (subadult). The limb shows an appearance closely similar to that of the adult. The zp/ap ratio (1.36; Table 5) indicates a zeugopodium of length even greater than the autopodium length of previous stages. Except for the fibula, which still exhibits the proximal epiphysis not fused to its diaphysis, all the elements of the limb are completely ossified (Table 2).

Zeugopodium. The distal epiphysis of the tibia is fused to its diaphysis, marking the end of ossification for this element (Fig. 4C,D and Table 2). The distal epiphysis of the fibula is fused to its diaphysis (Fig. 4C,D).

Autopodium. At the basipodium level, cuneiform I ventral sesamoid is completely ossified (Fig. 4D and Table 3). At the acropodium level, the *Ossa sesamoidea dorsalia* at all the proximal and medial phalanges are completely ossified (Fig. 4C and Table 3).

Stage H (adult). The final configuration of the adult shows a markedly slender appearance of the hindlimb; the zp/ap ratio (1.46, Table 5) indicates a zeugopodium that significantly exceeds the autopodium length. The proximal epiphysis of the fibula is now fused to its diaphysis, marking the end of ossification for this element (Fig. 5A,C and Table 2). All bones are completely ossified and bone processes are fully developed and articulated closely with associated bony elements. F5

Comparative Hindlimb Morphology in Adults of *D. rotundus*, *A. lituratus*, and *M. molossus*

The zp/ap ratio of the adults is bigger in *D. rotundus* (1.46) than in *M. molossus* (1.39) and *A. lituratus* (1.35); this characteristic gives the common vampire bat a slender hindlimb appearance with respect to the other two species, with a zeugopodium considerably bigger than the autopodium (Fig. 5 and Table 6). T6

Zeugopodium. *M. molossus* and *A. lituratus* exhibit a very thin fibula compared to the other elements of its hindlimbs; in *M. molossus* the fibula looks like a complete and arched bone along the tibia, whereas in *A. lituratus* it is incomplete, extending parallel and straight from the distal tip of the tibia up to 4/5 of its length. Meanwhile, *D. rotundus* presents a complete and robust fibula, extending parallel and straight along the tibia with a thickness similar to the latter (Fig. 5 and Table 6).

In *D. rotundus*, distally, the fibula articulates with the tibia, the talus and calcaneus (Fig. 5B), whereas in *A. lituratus* and *M. molossus*, it articulates only with the tibia and the talus (Fig. 5F,J and Table 6). The tibia and fibula of *A. lituratus* and *M. molossus* lack the characteristic T-shaped cross section exhibited by *D. rotundus*, since the latter possesses an already described pair of deep grooves along each element (Fig. 5A,C and Table 6). The tibia of *A. lituratus* exhibits a ventral sesamoid on its distal epiphysis that is absent in the other two species (called here as tibial ventral sesamoid; Fig. 5L and Table 6).

Fig. 5. Comparative hindlimb morphology in adults of species with different terrestrial locomotion capabilities. A, dorsal; B, dorsal detail; C, ventral, and D, ventral detail views of D. rotundus. E, dorsal; F, dorsal detail; G, ventral, and H, ventral detail views of Molossus molossus. I, dorsal; J, dorsal detail; K, ventral, and L, ventral detail views of Artibeus lituratus. Abbreviations: cal, calcar; cdp, calcaneous dorsal process; cds, calcaneous dorsal sesamoid; cmp, calcaneous medial process at the Tuber calcanei; culs, cuneiform I ventral sesamoid; dfa, distal fibular articulation; fdg, fibular dorsal groove; fi, fibula; fvg, fibular ventral groove; mVp, metatarsal V process; mVs, metatarsal V ventral sesamoid; nvp, navicular ventral process; osd, Ossa sesamoidea dorsalia; osm, Os sesamoideum metatarsale; osp, Ossa sesamoidea proximalia; tavs, talus ventral sesamoid; tc, Tuber calcanei; tdp, talus dorsal process; tds, talus dorsal sesamoid; tmg, tibial medial groove; tvg, tibial ventral groove; tvs, tibial ventral sesamoid.

ID: **jwweb3b2server** Time: 14:51 I Path: D:/Wiley/Support/XML_Signal_Tmp_AA/JW-AR##170103

J_ID: AR Customer A_ID: AR23646 Cadmus Art: AR23646 Ed. Ref. No.: AR-17-0026.R1 Date: 8-August-17 Stage: Page: 12

Autopodium. At the basipodium level, the proximal dorsum of the talus of *D. rotundus* and *M. molossus* possesses the talus dorsal process, which extends medially articulating with the calcaneus; this process is absent in *A. lituratus* (Fig. 5B,F and Table 6). The three species present the *Tuber calcanei* process at the calcaneus, a proximal and medial process that extends medially as a spur-shaped projection (Fig. 2B,F,J and Table 6). In *M. molossus* and *A. lituratus* exists a proximal and medial concave process of the calcaneus at the *Tuber calcanei*, whereby the calcar bone articulates (called here as calcaneous medial process at the *Tuber calcanei*); this process is very pronounced in *M. molossus*, less marked in *A. lituratus* and absent in *D. rotundus* (Fig. 5F,J and Table

TABLE 6. Comparison of hindlimb bone characters among three bat species with different terrestrial locomotion capabilities

			Species		
Region	Bony elements	Characters	*Desmodus rotundus* (nimble walker)	*Molossus molossus* (erratic walker)	*Artibeus lituratus* (non-walker)
Zeugopodium	Tibia	Tibial medial and tibial ventral grooves.*	✓	x	x
		Tibial ventral sesamoid.*	x	x	✓
	Fibula	Fibular dorsal and fibular ventral grooves.*	✓	x	x
		Shape of the fibula.	Sturdy, nearly as thick as the tibia, complete, straight parallel along the tibia length	Thin, complete, describing an arch along the tibia length	Thin, incomplete, straight along the tibia length up to four fifths of this
		Distal fibular articulation.	Articulates with the tibia, talus, and calcaneus	Articulates with the tibia and the talus	Articulates with the tibia and the talus
Autopodium	Calcar	Shape of the calcar.	Sturdy (short and flattened), tab-like shaped	Thin and long up to three quarters of the zeugopodium length	Thin and long up to half of the zeugopodium length
		Consistence of the calcar.	Mostly chondral (two-thirds chondral)	Mostly bony (one quarter chondral)	Mostly chondral (a minimum bony portion at the base)
	Calcaneus	Tuber calcanei, medial and proximal process at the calcaneus.	✓	✓	✓
		Calcaneous medial process at the Tuber calcanei.*	X	✓	✓
		Calcaneous dorsal process.*	✓	✓	x
		Calcaneous dorsal sesamoid.*	X	✓	x
	Talus	Talus dorsal process.*	✓	✓	x
		Talus dorsal sesamoid.*	X	✓	x
		Talus ventral sesamoid.*	X	x	✓
	Navicular	Navicular ventral process.*	✓	x	x
	Matatarsals	Ossa sesamoidea dorsalia, dorsal and distal on metatarsals II-V.	X	x	✓
		Ossa sesamoidea proximalia (paired), ventral and distal on metatarsals I–V.	✓	✓	✓
		Os sesamoideum metatarsale, ventral and proximal on metatarsal III.	X	✓	x

ID: jwweb3b2server Time: 14:51 I Path: D:/Wiley/Support/XML_Signal_Tmp_AA/JW-AR##170103

J_ID: AR Customer A_ID: AR23646 Cadmus Art: AR23646 Ed. Ref. No.: AR-17-0026.R1 Date: 8-August-17 Stage: Page: 13

TABLE 6. (continued).

Region	Bony elements	Characters	Species: *Desmodus rotundus* (nimble walker)	Species: *Molossus molossus* (erratic walker)	Species: *Artibeus lituratus* (non-walker)
		Metatarsal V proximal process.*	✓	✓	✓ barely noticeable
		Metatarsal V ventral sesamoid.*	✓	x	x
	Cuneiforms	Cuneiform I ventral sesamoid.*	✓	✓	x
	Phalanges	Ossa sesamoidea dorsalia, dorsal and distal on proximal phalanx I/dorsal and proximal on medial phalanges II–V/dorsal and distal on medial phalanges II–V.	✓	x	✓
		zp/ap ratio.	1.46; conferring a slender appearance to the hindlimb	1.39; conferring a robust appearance to the hindlimb	1.35; conferring a robust appearance to the hindlimb

Check symbol indicates presence of a character, "x" indicates absence of a character. Sesamoids and bone processes without name given previously in the literature are indicated with asterisk. Zeugopodium/autopodium values are averages of the individual values for each species.

6). Furthermore, in *D. rotundus* and *M. molossus* the calcaneus exhibits a dorsal and latero-distal process (called here as calcaneous dorsal process); this process is very pronounced in *D. rotundus* (like a thick arc that extends laterally on the talus), less marked in *M. molossus* (like a projection that extends laterally and distally on part of the talus and the cuboid) and absent in *A. lituratus* (Fig. 5B,F and Table 6).

The calcar is different in the three species: it is long and fully ossified in *M. molossus*, long and mostly chondral in *A. lituratus*, and short, sturdy, mostly chondral and tab-like in *D. rotundus* (Fig. 5A,B,E,I and Table 6). The navicular of *D. rotundus* presents a ventral and proximal process that extends proximally over the ventral surface of the talus (navicular ventral process; Fig. 5D and Table 6). Dorsally, *M. molossus* presents a sesamoid on the distal tip of the talus (called here as talus dorsal sesamoid) and another on the distal tip of the calcaneus (called here as calcaneous dorsal sesamoid; Fig. 5F and Table 6); these sesamoids are absent in the other two species. Ventrally, *M. molossus* and *D. rotundus* present a sesamoid on cuneiform I (cuneiform I ventral sesamoid; Fig. 5D,H and Table 6), whereas *A. lituratus* presents a sesamoid on the proximal tip of the talus (called here as talus ventral sesamoid; Fig. 5L and Table 6).

At the metapodium level, in all the examined species the proximal epiphysis of metatarsal V presents a process that widens medially and laterally. This process is marked in *M. molossus* and *D. rotundus*, and barely noticeable in *A. lituratus* (metatarsal V proximal process; Fig. 5B,F,J and Table 6). Dorsally, *A. lituratus* presents the *Ossa sesamoidea dorsalia* as a single sesamoid on each distal epiphysis of metatarsals II–V; these sesamoids are absent in the other two species (Fig. 5I and Table 6). Ventrally, the three species present a pair of sesamoids on each distal epiphysis of metatarsals I–V, called *Ossa sesamoidea proximalia* (Fig. 5C,G,K and Table 6). Also ventrally, *D. rotundus* presents a sesamoid on the proximal epiphysis of metatarsal V, which is absent in the other two species (metatarsal V ventral sesamoid; Fig. 5C,D and Table 6), whereas *M. molossus* presents one on the proximal epiphysis of metatarsal III, called *Os sesamoideum metatarsale*, which is absent in the other two species (Fig. 5H and Table 6).

At the acropodium level, in both *A. lituratus* and *D. rotundus* the *Ossa sesamoidea dorsalia* appears as a single sesamoid on each proximal epiphysis of medial phalanges II–V, on the distal epiphysis of proximal phalanx I and on the distal epiphysis of medial phalanges II–V; these sesamoids are absent in *M. molossus* (Fig. 5A,I and Table 6).

DISCUSSION

Postnatal Development of Hindlimbs in *D. rotundus*

The autopodium of the newborn *D. rotundus* is a well-developed structure that has already reached 84% of its adult length (Table 5). At this stage, the autopodium represents 57% of the total lower hindlimb length (with a zp/ap ratio of 0.74; Fig. 1A,B and Table 5), being outgrown gradually by the zeugopodium during postnatal development, to represent about 41% of the total lower hindlimb length at the adult H stage (with a zp/ap ratio of 1.46; Fig. 5A,C and Table 5). Despite the specializations for terrestrial locomotion, the relationship between newborn autopodium length and the total lower hindlimb length in *D. rotundus* (57%) is consistent with values reported for newborns of *M. lucifugus* (60%; Adams, 1992), *Artibeus jamaicensis* (53%), *Rousettus celebensis* (61%) and *Megaloglossus woermanni* (62%; Adams and

J_ID: AR Customer A_ID: AR23646 Cadmus Art: AR23646 Ed. Ref. No.: AR-17-0026.R1 Date: 8-August-17 Stage: Page: 14

Thibault, 2000). Previous studies related this advanced developmental condition of the newborn autopodium (almost similar in length to the adult autopodium) to an earlier prenatal onset of ossification with respect to other boreoeutherians (Laurasiatheria and Euarchontoglires; Koyabu and Son, 2014). Such condition is related to functional requirements to attach to the mother or roost using their hindlimbs (Orr, 1970; Farnum et al., 2007; Koyabu and Son, 2014). During the walk process in *D. rotundus*, the propulsion phase occurs via extension of the knee, with the autopodium being positioned in posterior direction and in contact with the ground, whereas in the opposite hindlimb the knee is contracting and the autopodium is moving anteriorly (Altenbach, 1979). Zeugopodium length is important during this process, since it determines the distance of the step taken with the hindlimb during walk process. The variation of the zeugopodium/autopodium ratio during development reflects functional needs pointed to an optimal displacement.

The ossification onset events of the hindlimb autopodium in recently studied bats follow a distal to proximal directional sequence (phalanges, metatarsals and tarsals; Koyabu and Son, 2014). As a conservative condition, *D. rotundus* shows a similar distal to proximal sequence pattern for the ossification completion events (bones completely ossified, including the closure of secondary ossification centres, if present) during postnatal development: distal phalanges (prenatally), medial phalanges (juvenile B stage), proximal phalanges, metatarsals (juvenile C stage), tarsals (juvenile D stage), calcar (juvenile E stage), tibia (subadult G stage) and fibula (adult H stage) (Figs. 1–5 and Table 2).

The ossification onset of the calcar of *D. rotundus* at the middle juvenile D stage (Fig. 3A,B), followed by the ossification completion at the subsequent late juvenile E stage (Fig. 3C,D and Table 2), are similar to those reported for *Myotis lucifugus*, beginning and ending ossification at late juvenile stages (Adams, 1992). In contrast, calcar ossification in *A. jamaicensis* starts and ends before birth (Adams and Thibault, 2000). However, such differences in the ossification timing of the calcar are not surprising, considering the morphological and functional diversity of this structure (Schutt and Simmons, 1998; Adams and Thibault, 2000).

The proximal extra ossification centre at the calcaneus of *D. rotundus* is the precursor of the *Tuber calcanei* process (Fig. 2A,B and Table 4); this process seems to constitute a traction epiphysis whereby the *m. gastrocnemius* tendon is inserted. Traction epiphyses are projections present in some bone epiphyses of mammals and birds into which a tendon is inserted and involved in mechanical movements (Parsons, 1904). Such ossifications are originated by the fusion of a pre-existing intratendinous sesamoid to the bone during evolution, showing a separate ossification centre during development (Parsons, 1904, 1905, 1908; Barnett and Lewis, 1958; Eyal et al., 2015).

The sesamoids present in the hindlimb of *D. rotundus* starts ossification at different postnatal stages (between early juvenile B and early subadult F), all of them ending ossification at subadult F and G stages (except for metatarsal V ventral sesamoid; Table 3). A similar pattern is observed in the formation of hindlimb bone processes, which determine the final adult shape of bones. The formation of these bone processes starts when ossification of most hindlimb elements ends (between early juvenile B and middle juvenile D stages; Tables 2 and 4), and half of them ends formation at the subadult F stage (Table 4). Additionally, the zp/ap ratio shows a progressively increasing difference between regions (favoring zeugopodium length) since the subadult F stage (Table 5). Such development timings are consistent with those reported by Reyes-Amaya and Jerez (2013) for this species, in which cranial suture closure and bone process completion occur at subadult F and G stages, coinciding with the beginning of the independent life of *D. rotundus* (Table 1). During this period, individuals begin to feed without parental accompaniment (~4 months after birth; Schmidt et al., 1980). These results suggest the functional nature of the bone processes, sesamoids and zp/ap proportions developed in the hindlimb of *D. rotundus* at subadult F and G stages (Tables 3, 4, and 5), linked to a good terrestrial locomotion and in turn associated with the feeding process of this specialized sanguivorous species (see below).

Comparative Hindlimb Morphology in Adults of *D. rotundus*, *A. lituratus*, and *M. molossus*

The comparisons of the morphological characters of the adult hindlimb among evaluated species with different terrestrial locomotion capabilities (Table 6) reveal a set of four characters concentrated at the autopodium of the two walking bats, *D. roundus* (nimble walker) and *M. molossus* (erratic walker), which are absent in the non-walker *A. lituratus*: (1) A well-developed metatarsal V proximal process, widening the proximal epiphysis of metatarsal V toward both lateral and medial sides (Fig. 5B,F). This bone process is linked to a further development of the *m. peroneus brevis* and *m. abductor digiti quinti*, whose function is to flex and rotate the foot, and abduct the fifth digit (Vaughan, 1959). (2) The presence of cuneiform I ventral sesamoid (Fig. 5D,H), associated with greater mechanical stress on the plantar surface of the hindlimb autopodium during terrestrial movements (Sarin et al., 1999; Sarin and Carter, 2000). (3)The presence of the talus dorsal process, which extends medially joining the calcaneus (Fig. 5B,F), and (4) The presence of the calcaneous dorsal process, which extends laterally joining the talus Fig. 5B,F). The last two conferring a greater stability to the hindlimbs of these species during terrestrial locomotion.

In addition, a set of seven characters distributed along the hindlimb of the nimble walker *D. rotundus* were detected, which are absent in the other two species evaluated (Table 6): (1) the distal articulation of the fibula with the tibia, talus and calcaneus (rather than only with the tibia and talus found in the other two species; Fig. 5B) and (2) presence of the navicular ventral process extending proximally over the talus (Fig. 5D). These characters are associated with a greater tight articulation between bony elements in *D. rotundus*, granting more stability to the hindlimbs during terrestrial locomotion. The characters (3) robustness of the fibula (nearly as thick as the tibia) and (4) presence of deep grooves along the tibia and fibula (Fig. 5A,C and Table 6) are associated with an increasing surface of the shafts in *D. rotundus*, related with the development of its associated muscles (Vaughan, 1970). The *m. extensor hallucis longus* (tibial extensor group) moves the hindlimb

ID: jwweb3b2server Time: 14:51 I Path: D:/Wiley/Support/XML_Signal_Tmp_AA/JW-AR##170103

J_ID: **AR** Customer A_ID: **AR23646** Cadmus Art: **AR23646** Ed. Ref. No.: **AR-17-0026.R1** Date: **8-August-17** Stage: Page: **15**

autopodium forward, increasing the length and effectiveness of the stride. The *m. peroneus longus* and *m. peroneus brevis* (peroneal group) pull the foot laterally, bringing it into line with the hindlimb, thus giving a final push at the end of the propulsion stroke of the stride. Finally, the *m. gracilis* (adductor group) acts as a flexor and adductor of the hindlimb, working during forward component of the stride and supporting the weight during the propulsion stroke of the stride (Vaughan, 1959). A previous hypothesis proposed a thinning of the tibia–fibula complex (zeugopodium) in most bats as a derived condition, associated with the hanging posture as an adaptation for flight that hampers terrestrial mobility (Howell and Pylka, 1977). Although mechanical studies rejected such hypothesis by demonstrating that a non-walker bat (*Pteronotus parnellii*) wielded greater forces on the hindlimbs during walking than two walker bats (*D. rotundus* and *Diaemus youngi*; Riskin et al., 2005), the further development of the muscles associated with the robust and grooved shafts of the tibia and fibula in *D. rotundus*, suggests an important character dealing with mechanical forces produced during terrestrial locomotion. (5) A bigger zp/ap ratio (1.46) than in *M. molossus* (1.39; erratic walker) and *A. lituratus* (1.35; non-walker) (Fig. 5A,C and Table 6). This difference could be associated with mechanical advantage favoring the common vampire bat, with higher force arm during walking with a slender hindlimb (considering hindlimbs and associated muscles as a lever system; Johnson and Hurley, 2003). This assumption should be tested using biomechanical models. However, the advantage can be suggested based on the locomotion model described by Altenbach (1979) for *D. rotundus*, in which the length of the zeugopodium represents the distance of the step taken with the hindlimb by extending the knee. (6) A small tab-like and mostly chondral calcar, without the presence of the calcaneus process at the *Tuber calcanei* articulating with it (Fig. 5A,B and Table 6) and associated with a rudimentary uropatagium. Functional inferences for the calcar seem to be relevant, taking into account that its size, shape and composition (bone or cartilage) exhibit considerable variation among bats; the calcar is well developed in insectivorous, frugivorous and carnivorous species that use both the calcar and uropatagium for food handling (Schutt and Simmons, 1998). Accordingly, *A. lituratus* and *M. molossus* showed a well developed calcar, completely ossified in the former (insectivorous) and mostly chondral in the latter (frugivorous), articulating with the calcaneous medial process at the *Tuber calcanei* (Fig. 5E,I and Table 6), and associated with a developed uropatagium. The reductions of the calcar and uropatagium in *D. rotundus* with respect to the other two species evaluated seem to be advantageous during nimbly terrestrial locomotion, preventing the friction of these structures. The small proximal ossification in the long calcar of *A. lituratus* and the sturdy tab-like calcar of *D. rotundus* contrast with the report of Schutt and Simmons (1998), who suggest the calcar is completely chondral in these two species. The proximal ossification of the calcar of *A. lituratus* is in agreement with that reported for *A. jamaicensis* (Adams and Thibault, 2000). The long and completely ossified calcar of *M. molossus* is consistent with that reported by Schutt and Simmons (1998). Finally, (7) presence of metatarsal V ventral sesamoid. Sesamoid bones seem to be a result of mechanical stress, since its formation during development responds to a threshold of mechanical load (Sarin et al., 1999; Sarin and Carter, 2000). However, sesamoid precursors are present at early embryonic development of some amniotes (Jerez et al., 2010) and anamniotes (Abdala and Ponssa, 2012), before mechanical forces could represent a determining influence on these structures. In this report, four out of nine sesamoids identified in the species evaluated are exclusively present in *D. rotundus* (nimble walker) or *M. molossus* (erratic walker) (Table 6). These facts suggest the correlation of sesamoids with the level of terrestrial ability in these species, reinforcing the hypothesis that although formation of sesamoid precursors is genetically controlled and possibly inherited, the extrinsic stimulus of mechanical stress drives its following differentiation according to the ecological behavior of species (Sarin and Carter, 2000; Doherty, 2007; Jerez and Tarazona, 2009; Doherty et al., 2010; Eyal et al., 2015; Regnault et al., 2016).

The particular morphological characters described occurring during *D. rotundus* postnatal development provide some insights of the ontogenetic variation of traits linked to a nimbly terrestrial locomotion in adults of this species: (1) distal articulation of the fibula with the tibia, talus and calcaneus; (2) presence of the navicular ventral process (Fig. 5D); (3) fibula nearly as robust as tibia; (4) presence of deep grooves along tibia and fibula (Fig. 5A,C); (5) bigger zp/ap ratio than in the other studied species (Table 6); (6) reduced tab-like and mostly chondral calcar (Fig. 5A,B); and (7) presence of metatarsal V ventral sesamoid. However, those characters shared by adults of *D. rotundus* and *M. molossus* apparently linked to terrestrial locomotion suggest convergent evolution processes, considering that the ability of walking has evolved independently in some lineages of bats (Riskin et al., 2006; Hand et al., 2009; Riskin et al., 2016): (1) presence of a well-developed metatarsal V proximal process; (2) presence of cuneiform I ventral sesamoid (Fig. 5D,H); (3) presence of the talus dorsal process (Fig. 5B,F); and (4) presence of the calcaneous dorsal process (Fig. 5B,F). Accordingly, it could be also expected that other bats with good or intermediate terrestrial locomotion capabilities, such as *Mystacina tuberculata* (Hand et al., 2009), may share some of the morphological characters described here for *D. rotundus* and *M. molossus*, as part of convergent evolution processes. Further analyses should be conducted including a more speciose taxonomic sample including species with different life histories, in order to determine the relationship between form and function during the development of the bat hindlimb, as well as the evolutionary view of ossification events.

ACKNOWLEDGEMENTS

The authors thank the curators H. López-Arévalo (Alberto Cadena Garcia Mammal Collection, Instituto de Ciencias Naturales—ICN, Universidad Nacional de Colombia, sede Bogotá—UN) and Pablo Teta (Mammal Collection, Museo Argentino de Ciencias Naturales Bernardino Rivadavia—MACN), for providing access to specimens, and three anonymous reviewers, for providing comments that substantially improved the manuscript. The authors dedicate this study to the peace treaty reached between the FARC rebels and the Colombian government, as an

encouragement for the Colombian people to keep walking forward to a definitive peace with social justice.

LITERATURE CITED

Abdala V, Ponssa ML. 2012. Life in the slow lane: The effect of reduced mobility on tadpole limb development. Anat Rec 295:5–17.

Adams RA. 1992. Stages of development and sequence of bone formation in the little brown bat, *Myotis lucifugus*. J Mammal 73: 160–167.

Adams RA. 2008. Morphogenesis in bat wings: Linking development, evolution and ecology. Cells Tissues Organs 187:13–23.

Adams RA, Shaw J. 2013. Time's arrow in the evolutionary development of bat flight. In: Adams RA, Pedersen SC, editors. Bat evolution, ecology and conservation. New York: Springer. p 21–46.

Adams RA, Thibault KM. 2000. Ontogeny and evolution of the hindlimb and calcar: Assessing phylogenetic trends. In: Adams RA, Pedersen SC, editors. Ontogeny, functional ecology, and evolution of bats. New York: Cambridge University Press. p 316–332.

Altenbach JS. 1979. Locomotor morphology of the vampire bat, *Desmodus rotundus*. Spec Publ Am Soc Mammal 6:1–137.

Baker RJ, Bininda-Emonds ORP, Mantilla-Meluk H, Porter CA, Van Den Bussche RA. 2012. Molecular timescale of diversification of feeding strategy and morphology in new world leaf-nosed bats, Phyllostomidae: A phylogenetic perspective. In: Gunnell GF, Simmons NB, editors. Evolutionary history of bats: Fossils, molecules and morphology. New York: Cambridge University Press. p 385–409.

Barnett CH, Lewis OJ. 1958. The evolution of some traction epiphyses in birds and mammals. J Anat 92:593–601.

Doherty ARH. 2007. Murine metapodophalangeal sesamoid bone mineralization: A light and electron microscopy study. Unpublished Master Thesis. Ohio: Kent State University. 78 pp.

Doherty E, Lowder M, Jacquet RD, Landis WJ. 2010. Murine metapodophalangeal sesamoid bones: Morphology and potential means of mineralization underlying function. Anat Rec 293:775–785.

Eyal S, Blitz E, Shwartz Y, Akiyama H, Ronen S, Zelzer E. 2015. On the development of the patella. Development 142:1831–1839.

Farnum CE, Tinsley M, Hermanson JW. 2007. Forelimb versus hindlimb skeletal development in the big brown bat, *Eptesicus fuscus*: Functional divergence is reflected in chondrocytic performance in autopodial growth plates. Cells Tissues Organs 187:35–47.

Ferrarezzi H, Gimenez EA. 1996. Systematic patterns and the evolution of feeding habits in Chiroptera (Archonta: Mammalia). J Comp Biol 1:75–94.

Greenhall AM, Schmidt U. 1988 Natural history of vamire bats. Boca Raton: CRC Press.

Hand SJ, Weisbecker V, Beck RDM, Archer M, Godthel H, Tennyson AJD, Worthy TH. 2009. Bats that walk: A new evolutionary hypothesis for the terrestrial behaviour of New Zealand's endemic mystacinids. BMC Evol Biol 9:169.

Howell DJ, Pylka J. 1977. Why bats hang upside down: A biomechanical hypothesis. J Theor Biol 69:625–631.

Jerez A, Mangione S, Abdala V. 2010. Occurrence and distribution of sesamoid bones in squamates: A comparative approach. Acta Zool 91:295–305.

Jerez A, Tarazona OA. 2009. Appendicular skeleton in *Bachia bicolor* (Squamata: Gymnophthalmidae): Osteology, limb reduction and postnatal skeletal ontogeny. Acta Zool 90:42–50.

Johnson AT, Hurley BF. 2003. Factors affecting mechanical work in humans. In: Schneck D, Bronzino JD, editors. Biomechanics: Principles and applications. Boca Ratón: CRC Press. p 152–161.

Koyabu D, Son NT. 2014. Patterns of postcranial ossification and sequence heterochrony in bats: Life histories and developmental trade-offs. J Exp Zool B Mol Dev Evol 322:607–618.

MacAlister A. 1872. The myology of the Cheiroptera. Philos T R Soc B 162:125–171.

Mollerach M, Mangione S. 2004. Adaptaciones morfológicas de la lengua de *Desmodus rotundus* (Chiroptera: Phyllostomidae) en función de la alimentación. Mast Neotrop 11:203–209.

Nomina Anatomica Veterinaria. 2012. Hannover: Editorial Committee of the International Committee on Veterinary Gross Anatomical Nomenclature. 5th ed. (revised version). Hannover (Germany): Editorial Committee, World Association of Veterinary Anatomists. 177 pp.

Orr RT. 1970. Development: Prenatal and postnatal. In: Wimsatt W, editor. Biology of bats. New York: Academic Press. p 217–231.

Parsons FG. 1904. Observations on traction epiphyses. J Anat Physiol 38:248–258.

Parsons FG. 1905. On pressure epiphyses. J Anat Physiol 39: 402–412.

Parsons FG. 1908. Further remarks on traction epiphyses. J Anat Physiol 42:388–396.

Regnault S, Jones MEH, Pitsillides AA, Hutchinson JR. 2016. Anatomy, morphology and evolution of the patella in squamate lizards and tuatara (*Sphenodon punctatus*). J Anat 228:864–876.

Reyes-Amaya N, Jerez A. 2013. Postnatal cranial ontogeny of the common vampire bat *Desmodus rotundus* (Chiroptera: Phyllostomidae). Chirop Neotrop 19:1198–1211.

Riskin DK, Bertram JE, Hermanson JW. 2005. Testing the hindlimb-strength hypothesis: Non-aerial locomotion by Chiroptera is not constrained by the dimensions of the femur or tibia. J Exp Biol 208:1309–1319.

Riskin DK, Bertram JEA, Hermanson JW. 2016. The evolution of terrestrial locomotion in bats. In: Bertram JEA, editor. Understanding mammalian locomotion: Concepts and applications. Hoboken: Wiley. p 307–324.

Riskin DK, Hermanson JW. 2005. Independent evolution of running in vampire bats. Nature 434:292.

Riskin DK, Parsons PE, Schutt WA Jr, Carter GG, Hermanson JW. 2006. Terrestrial locomotion of the New Zealand short-tailed bat, *Mystacina tuberculata*, and the common vampire bat, *Desmodus rotundus*. J Exp Biol 209:1725–1736.

Sarin VK, Carter DR. 2000. Mechanobiology and joint conformity regulate endochondral ossification of sesamoids. J Orthop Res 18:706–712.

Sarin VK, Erickson GM, Giori NJ. 1999. Coincident development of sesamoid bones and clues to their evolution. Anat Rec 257:174–180.

Schaller O. 2007. Illustrated veterinary anatomical nomenclature. 3rd ed. Stuttgart: Enke Verlag. 625 pp.

Schmidt C, Schmidt U, Manske U. 1980. Observations of the behavior of orphaned juveniles in the common vampire bat (*Desmodus rotundus*). In: Wilson DE, Gardner AL, editors. Proceedings of the Fifth International Bat Research Conference. Lubbock: Texas Tech Press. p 105–111.

Scholey KD. 1986. The evolution of flight in bats. In: Nachtigall W, editor. Bat flight-Fledermausflug. New York: G. Fischer. p 1–12.

Schutt WA Jr. 1993. Digital morphology in the Chiroptera: The passive digital lock. Acta Anat 148:219–227.

Schutt WA Jr, Altenbach JS, Chang YH, Cullinane DM, Hermanson JW, Muradali F, Bertram JEA. 1997. The dynamics of flight-initiating jumps in the common vampire bat *Desmodus rotundus*. J Exp Biol 200:3003–3012.

Schutt WA Jr, Simmons NB. 1998. Morphology and homology of the chiropteran calcar, with comments on the relationships of Archaeopteropus. J Mamm Evol 5:1–32.

Sears KE, Behringer RR, Rasweiler JJIV, Niswander LA. 2006. Development of bat flight: Morphologic and molecular evolution of bat wing digits. Proc Natl Acad Sci USA 103:6581–6586.

Vaughan TA. 1959. Functional morphology of three bats: Eumops, Myotis, Macrotus. U Kansas Publ Mus Nat Hist 12:1–153.

Vaughan TA. 1970. The skeletal system. In: Wimsatt WA, editor. Biology of bats. New York: Academic Press. p 97–138.

Walton DW, Walton GM. 1970. Post-cranial osteology of bats. In: Slaughter R, Walton D, editors. About bats. Dallas: Southern Methodist University Press. p 93–125.

Wassersug RJ. 1976. A procedure for differential staining of cartilage and bone in whole formalin fixed vertebrates. Stain Tech 51: 131–134.

Werner EE. 1999. Ecological experiments and a research program in community ecology. In: Resetarits WJ Jr, Bernardo J, editors. Experimental ecology. Oxford: Oxford University Press. p 3–26.